Food Chemistry 138 (2013) 998–1007

Contents lists available at SciVerse ScienceDirect

Food Chemistry

journal homepage: www.elsevier.com/locate/foodchem

# Simultaneous detection of multiple adulterants in dry milk using macro-scale Raman chemical imaging

Jianwei Qin, Kuanglin Chao *, Moon S. Kim

*Environmental Microbial and Food Safety Laboratory, Henry A. Wallace Beltsville Agricultural Research Centre, Agricultural Research Service, United States Department of Agriculture, 10300 Baltimore Ave., Beltsville, MD 20705, USA*

ARTICLE INFO

*Article history:*
Received 30 April 2012
Received in revised form 2 October 2012
Accepted 23 October 2012
Available online 12 November 2012

*Keywords:*
Raman imaging
Quality and safety
Milk
Adulterant
Mixture analysis

ABSTRACT

The potential of Raman chemical imaging for simultaneously detecting multiple adulterants in milk powder was investigated. Potential chemical adulterants, including ammonium sulphate, dicyandiamide, melamine, and urea, were mixed together into skim dry milk in the concentration range of 0.1–5.0% for each adulterant. Using a 785-nm laser, a Raman imaging system acquired hyperspectral images in the wavenumber range of 102–2538 $cm^{-1}$ for a 25 × 25 $mm^2$ area of each mixture sample, with a spatial resolution of 0.25 mm. Self-modelling mixture analysis (SMA) was used to extract pure component spectra, by which the four types of the adulterants were identified at all concentration levels based on their spectral information divergence values to the reference spectra. Raman chemical images were created using the contribution images from SMA, and their use to effectively visualise identification and spatial distribution of the multiple adulterant particles in the dry milk was demonstrated.

Published by Elsevier Ltd.

## 1. Introduction

The capacity for rapid and accurate authentication of food ingredients is an important part of food safety programs, as illustrated by several incidents of adulteration of products such as milk and wheat gluten. In 2007, the widespread recall of pet foods occurred after thousands of dogs and cats in the US experienced kidney failure. The US Food and Drug Administration (FDA) later determined that a wheat gluten ingredient, purchased from a particular Chinese source by some American and Canadian pet food manufacturers, was contaminated with melamine. In 2008, thousands of Chinese children experienced kidney problems, including several fatal cases, as a result of melamine adulteration of infant formula produced by a major Chinese dairy company, leading to a recall of 700 tonnes of the formula product. Although none of the adulterated Chinese formula was found in the US in 2008, the FDA still expressed concern for the US market since contaminated Chinese product had been found at a US store during a similar incident in 2004 that involved milk adulteration by urea, soap powder, and starch components.

Generally, the motivation to add adulterants such as melamine to milk powder or wheat gluten was to produce an increased nitrogen content of the food as perceived by conventional testing methods, because nitrogen content is used to estimate protein content of foods. The Kjeldahl method is the standard method used worldwide for measuring nitrogen in protein food, and involves reacting the food protein to produce ammonium sulphate (among other reaction products)—ammonia is then captured and quantified by back titration. In 2008, the Chinese infant formula manufacturers added melamine to their infant formula in order to meet minimum protein requirements. A 3.1-g addition of melamine can be dissolved in 1 L of milk at room temperature without any precipitate, and can result in an overestimation of the protein content of the milk by as much as 30% (Hau, Kwan, & Li, 2009). Due to its greater solubility in warm water, melamine can be added in even greater amounts to dry milk powder since that product is usually reconstituted using warm water.

Current laboratory methods based on mass spectrometry, such as GC-MS and LC-MS/MS, can detect trace amounts of adulterants. These time-consuming procedures are expensive and can require labour-intensive preparation of samples as well as chemical extraction and filtration steps. Thus they are poorly suited for screening of large-volume food samples despite their accurate measurement results. Development of nondestructive detection methods for adulterants and/or contaminants, which can be performed rapidly and at lower cost, is becoming increasingly important for reasons of food safety and public health and also for the economic aspects of preventing product fraud. A potential alternative to chemistry-based laboratory methods is the use of Raman spectroscopy-based technique, given the specificity of the Raman signals that is possible for identifying chemical components and

* Corresponding author. Address: USDA/ARS/EMFSL, Bldg. 303, BARC-East, 10300 Baltimore Ave., Beltsville, MD 20705-2350, USA. Tel.: +1 301 504 8450/260; fax: +1 301 504 9466.
*E-mail address:* kevin.chao@ars.usda.gov (K. Chao).

0308-8146/$ - see front matter Published by Elsevier Ltd.
http://dx.doi.org/10.1016/j.foodchem.2012.10.115

the minimal sample preparation needed for the measurement. Raman spectroscopy has been used to detect adulterants in dry milk, such as melamine (Okazaki, Hiramatsu, Gonmori, Suzuki, & Tu, 2009; Qin, Chao, & Kim, 2010), whey (Almeida, Oliveira, Stephani, & de Oliveira, 2011), ammonium sulphate, dicyandiamide, and urea (Chao, Qin, Kim, & Mo, 2011). It has also been used to analyse nutritional parameters (e.g., fat, protein, and carbohydrate) of the milk powder (McGoverin, Clark, Holroyd, & Gordon, 2010; Moros, Garrigues, & de la Guardia, 2007). Besides Raman spectroscopy, other techniques, such as near-infrared (NIR) spectroscopy (Borin, Ferrao, Mello, Maretto, & Poppi, 2006; Lu et al., 2009) and nuclear magnetic resonance (NMR) spectroscopy (Belloque & Ramos, 1999; Hu, Furihata, Kato, & Tanokura, 2007), have also been investigated for milk composition analysis.

Raman chemical imaging applies the advantages of Raman spectroscopy to an imaging approach for screening large samples, allowing the presence and distribution of adulterants/contaminants within a food material to be visualised. Some Raman imaging instruments are commercially available but most perform measurements at microscale or nanoscale levels. The spatial range covered by such systems cannot satisfy the requirements of whole-surface inspection for individual food items. A Raman chemical imaging system was recently developed in our laboratory for macro-scale imaging of food and agricultural products (Qin et al., 2010), such as scanning cross-sections of cut tomatoes for maturity evaluation (Qin, Chao, & Kim, 2011).

Using this system, a research project was recently begun on authentication of dry milk and other food ingredients. The long-term goal of this line of investigation is to develop a macro-scale imaging-based Raman detection method for detecting adulterants and/or contaminants in powdered food and food ingredients. Our previous studies have demonstrated that Raman chemical imaging can be used to detect a single type of adulterant in the dry milk, using either a targeting approach (spectral information divergence for detecting melamine, Qin et al., 2010) or a non-targeting approach (self-modelling mixture analysis for separately detecting ammonium sulphate, dicyandiamide, and urea, Chao et al., 2011). Most other Raman-based research has also been limited to inspecting for one type of adulterant in one measurement. The capacity for detecting multiple adulterants from one sampling is desired since, in reality, more than one type of adulterant can be mixed into dry milk. To follow up on the previous investigations, this study aimed to develop a Raman chemical imaging method for simultaneous detection of multiple adulterants in dry milk powder. Specific objectives were to:

- Collect hyperspectral Raman images for mixtures of dry milk with four types of adulterants (i.e., ammonium sulphate, dicyandiamide, melamine, and urea);
- Develop mixture analysis algorithms for extracting and identifying Raman signals from different adulterants mixed into the milk powder; and
- Create Raman chemical images for visualising identification and spatial distribution of the multiple adulterant particles in the dry milk.

## 2. Materials and methods

### 2.1. Raman chemical imaging system

A point-scan Raman chemical imaging system was developed for macro-scale imaging of samples (Qin et al., 2010). A 16-bit CCD camera with $1024 \times 256$ pixels (Newton DU920N-BR-DD, Andor Technology, South Windsor, CT, USA) was used to acquire Raman scattering signals. A Raman imaging spectrometer (Raman Explorer 785, Headwall Photonics, Fitchburg, MA, USA) was mounted to the camera. The spectrometer accepts light through an input slit (5 mm long $\times$ 100 μm wide), and detects a Raman shift range of $-98$–$3998\ cm^{-1}$ (or a wavelength range of 799–1144 nm) with a spectral resolution of $3.7\ cm^{-1}$. A 785-nm laser module (I0785MM0350MF-NL, Innovative Photonic Solutions, Monmouth Junction, NJ, USA) served as the excitation source. The laser power at the sample surface was 170 mW, which was measured by a handheld power meter (NT54-018, Edmund Optics, Barrington, NJ, USA). A fibre optic Raman probe (RPB, InPhotonics, Norwood, MA, USA) was used to focus the laser and acquire Raman signals. A bifurcated fibre bundle was used to deliver the laser light to the probe and transfer the collected Raman signals to the spectrometer.

A two-axis motorized positioning table (MAXY4009W1-S4, Velmex, Bloomfield, NY, USA) was used to move the samples in two perpendicular directions, with a displacement resolution of 6.35 μm across a square area of $127 \times 127\ mm^2$. The Raman probe, the positioning table, and the sample materials were placed in a closed black box to avoid the influence of ambient light. The Raman imaging system was found to cover a wavenumber range of $102$–$2538\ cm^{-1}$ based on the result of spectral calibration using two Raman shift standards (i.e., polystyrene and naphthalene). System software was developed using LabVIEW (National Instruments, Austin, TX, USA) to fulfil functions such as camera control, data acquisition, sample movement, and synchronization. The 3-D Raman image data were saved in the format of Band Interleaved by Pixel (BIP), which can be analysed by commercial software packages such as ENVI (ITT Visual Information Solutions, Boulder, CO, USA). More detailed system description can be found in Qin et al. (2010).

### 2.2. Experimental samples and procedures

Chemical reagents—ammonium sulphate (>99.0%), dicyandiamide (>99.0%), melamine (>99.0%), and urea (>98.0%)—were obtained from Sigma-Aldrich (St. Louis, MO, USA). The reason for using ammonium sulphate was because it is one of the reaction products generated in the process of nitrogen measurement using the Kjeldahl method. Dicyandiamide and urea were selected because melamine is currently made most often from urea, and in the past was made from dicyandiamide. Organic skim dry milk (Organic Valley, La Farge, WI, USA) was purchased from a local supermarket. The four chemical reagents were mixed into the milk powder to make mixtures at six concentration levels for each adulterant (w/w): 0.1%, 0.2%, 0.5%, 1.0%, 2.0%, and 5.0%. These milk-plus-four-adulterant samples were contained in 50 ml polypropylene centrifuge tubes. A vortex mixer was used to shake and spin the tubes to ensure uniform distribution of the adulterant particles in the dry milk. Each sample was equally divided into three parts for imaging in triplicate. One mixture sample was also prepared by mixing homogenized whole-fat dry milk (Nestlé, Vevey, Switzerland) with the four chemical adulterants at a 0.1% concentration, to provide spectral comparison between homogenized and nonfat dry milk. In addition to the milk-adulterant mixtures, one sample was prepared by mixing together equal-weight fractions of all four chemical adulterants, without any dry milk powder, for the purpose of validating the algorithm for mixture analysis.

Petri dishes (Fisher Scientific, Pittsburgh, PA, USA) were used to hold the mixed powder samples. The diameter of each dish was 47 mm. The Raman imaging system scanned a $25 \times 25\ mm^2$ area for each sample using a CCD exposure time of 0.1 s and a step size of 0.25 mm for both X and Y directions, resulting in a $100 \times 100 \times 1024$ hypercube (1024 bands). Under these settings, the scan for each sample was finished in approximately 2 h. A dark current image was acquired with the laser off and a cap covering

the probe, and it was subtracted from the original sample image. Only the corrected images were used for further analysis. In addition to measurements for the mixture samples, the four chemical adulterants and the dry milk were each measured individually to provide reference Raman spectra. Lactose (99.5%, Sigma-Aldrich, St. Louis, MO, USA), a disaccharide sugar found in milk, was also measured to compare with the Raman spectrum of the dry milk.

### 2.3. Raman spectral and image analysis

The hyperspectral Raman images were analysed using self-modelling mixture analysis (SMA) to extract Raman signatures of different compositions. SMA uses an alternating least squares approach with added constraints to decompose a data matrix into the outer product of pure component spectra (or factors) and contributions (or scores). It is a useful tool to resolve a mixture of compounds without knowing the prior spectral information of the individual components (Vajna et al., 2011; Windig & Guilment, 1991). The hypercube of each sample was first unfolded in the spatial domain so that each single-band image became a vector. The 3-D image data ($100 \times 100 \times 1024$) was consequently reshaped to form a 2-D matrix ($10{,}000 \times 1024$), on which SMA can be performed in a same manner as that used for regular spectral data. After SMA, each score vector ($10{,}000 \times 1$) for the selected pure components was folded back to form a 2-D contribution image ($100 \times 100$) with same dimensions of the single-band image. SMA was conducted using the *Purity* function in PLS_Toolbox (Eigenvector Research, Wenatchee, WA, USA). An offset level of five was used in the *Purity* function. The *Purity* function gives a lower weight to variables with relatively small values through the parameter of offset. A percentage of the maximum for the mean of the data determines the offset value. Thus the offset level of five corresponds to a 5% × (maximum intensity) offset value in the original SMA method (Windig & Guilment, 1991).

Performing SMA requires the expected number of pure components to be pre-defined. For a mixture consisting of an unknown number of compositions, it is desirable to overestimate the number of the pure components, and then inspect the resolved spectra. Different numbers of pure components were tested for both the mixed-adulterants-only mixture and the milk-adulterant mixtures. The resolved spectra were examined to determine appropriate numbers of pure components to use. After the component spectra were extracted from the mixed samples, spectral information divergence (SID) was used to identify the adulterant type by evaluating the component spectra for similarities with the reference spectra of the four adulterants (i.e., ammonium sulphate, dicyandiamide, melamine, and urea). SID is a similarity metric that quantifies the difference between two spectra by utilizing the relative entropy to account for the spectral information. The smaller the SID value, the smaller the discrepancy between two spectra. Detailed algorithms for SID can be found in Chang (2000). For each pure component spectrum, four SID values were calculated using the four reference spectra of the adulterants. The component was identified as the adulterant that generated the least SID value.

The contribution maps corresponding to each identified adulterant were generated to illustrate the spatial distribution of the adulterant particles. For the sample mixed with the four chemical adulterants only, the classical least squares (CLS) method was used to create reference contribution maps using the reference spectra of the adulterants via the following linear model (Wise et al., 2006, chap. 6):

$$M = CR^T \quad (1)$$

where M is the matrix of the measured spectra ($10{,}000 \times 1024$), C is the matrix of the contributions ($10{,}000 \times 4$), and R is the matrix of the reference spectra ($1024 \times 4$). C can be determined using the pseudoinverse of R:

$$C = MR(R^TR)^{-1} \quad (2)$$

The contributions extracted from SMA were compared to the reference contributions from CLS to validate the algorithm for mixture analysis. For the contribution images of the milk-adulterant mixtures, a simple thresholding method was applied to create binary images of the individual adulterants. The binary images of the same sample were then combined to form chemical images of the multiple identified adulterants. The aforementioned data analysis procedures were executed using in-house programs developed in MATLAB (MathWorks, Natick, MA, USA).

## 3. Results and discussion

### 3.1. Reference Raman spectra of dry milk and chemical adulterants

Raman characteristics of dry milk and lactose in the wavenumber range of 102–2538 $cm^{-1}$ are shown in Fig. 1a. A fluorescence background, owing to the interaction of the 785-nm laser and the milk powder, was observed in the spectrum of the dry milk. Several small Raman peaks were found on the fluorescence baseline, of which five peaks can be attributed to the lactose since they share the same Raman shift positions (illustrated by the vertical lines in Fig. 1a). The peaks at other spectral positions are attributable to the proteins and other constituents in the dry milk (McGoverin et al., 2010). Fig. 1b shows the reference Raman spectra of

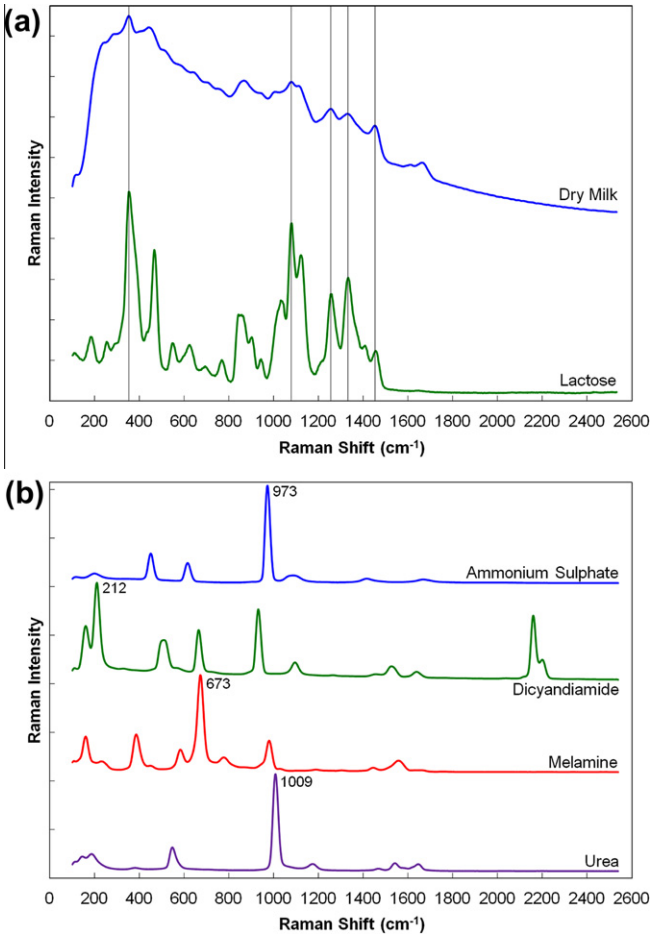


**Fig. 1.** Raman spectra of (a) skim dry milk and lactose and (b) four chemical adulterants.

the four chemical adulterants investigated in this study. A quick examination of their Raman spectra can reveal the similarities and differences among the chemical samples. Unlike the dry milk spectrum in Fig. 1a, all the adulterant spectra in Fig. 1b have a flat background due to the lack of the fluorescence signals. The Raman peaks of the four adulterants are generally located at different Raman shift positions. The highest peaks for ammonium sulphate, dicyandiamide, melamine, and urea were found at 973, 212, 673, and 1009 $cm^{-1}$, respectively. The corresponding wavenumbers are marked in the figure. Major Raman features for all the adulterants are located in the spectral region of 100–1700 $cm^{-1}$, with the exception of those for dicyandiamide which include two additional peaks around 2200 $cm^{-1}$. The differences among the Raman spectra of the adulterants formed the basis for detecting and distinguishing the chemical adulterants in the dry milk.

### 3.2. Self-modeling mixture analysis for mixed chemical adulterants

The Raman spectra from the reshaped 2-D matrix (10,000 × 1024) of the mixed-adulterants-only sample are shown in Fig. 2a. Similar to the spectra of the individual adulterants (Fig. 1b), all 10,000 spectra share a relatively flat baseline. The Raman peaks associated with the individual adulterants were also observed for the mixed-adulterants sample. The highest peaks for ammonium sulphate, dicyandiamide, melamine, and urea are marked in the figure. Raman images at these four peak positions (i.e., 212, 673, 973, and 1009 $cm^{-1}$) are shown in Fig. 2b. A single-band image at 1800 $cm^{-1}$ is also shown. All the images are displayed in the same intensity scale for the purpose of direct comparison. The images at the selected Raman peak positions exhibit different brightness patterns due to the wavenumber-dependent Raman scattering intensities and the spatial distribution of the adulterant particles. For example, the bright pixels in the 973 $cm^{-1}$ image are likely attributable to the particles of ammonium sulphate since its highest Raman peak appears at this wavenumber. The intensity of the 1009 $cm^{-1}$ image is lower than those of the images at other three peaks because of the relatively weak Raman signals from the urea particles. For the Raman shift positions that are lack of the Raman peaks (e.g., 1800 $cm^{-1}$), there are generally no notable features in the images.

Fig. 3 shows the results of the self-modelling mixture analysis for the mixed chemical adulterants. The pure component spectra extracted from SMA are plotted in Fig. 3a. The identification of each resolved spectrum was based on its spectral information divergence values with respect to the reference Raman spectra of the adulterants. For example, the SID values between the first extracted spectrum and the reference spectra of ammonium sulphate, dicyandiamide, melamine, and urea were 0.17, 0.99, 1.13, and 1.27, respectively. Thus this spectrum was identified as ammonium sulphate since it had the least spectral difference with ammonium sulphate. When compared to the reference spectra, the extracted pure component spectra retrieved almost all the spectral features (e.g., Raman peak positions and intensities) for each adulterant, demonstrating the effectiveness of SMA for recovering the individual chemical information from a mixture. The pure component spectra in Fig. 3a were the first four spectra extracted

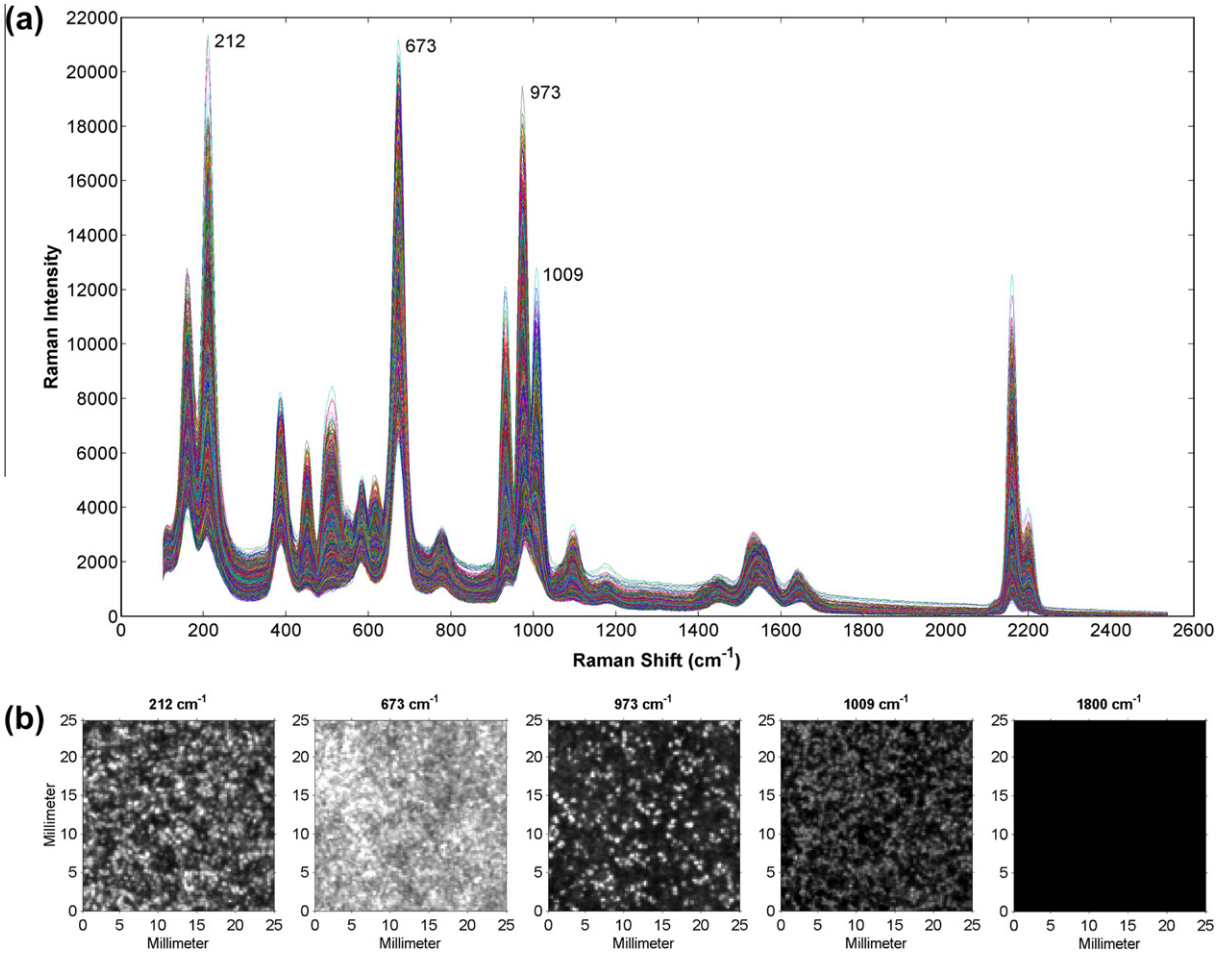


**Fig. 2.** Raman characteristics of mixed chemical adulterants (ammonium sulphate, dicyandiamide, melamine, and urea): (a) original spectra and (b) images at selected wavenumbers.

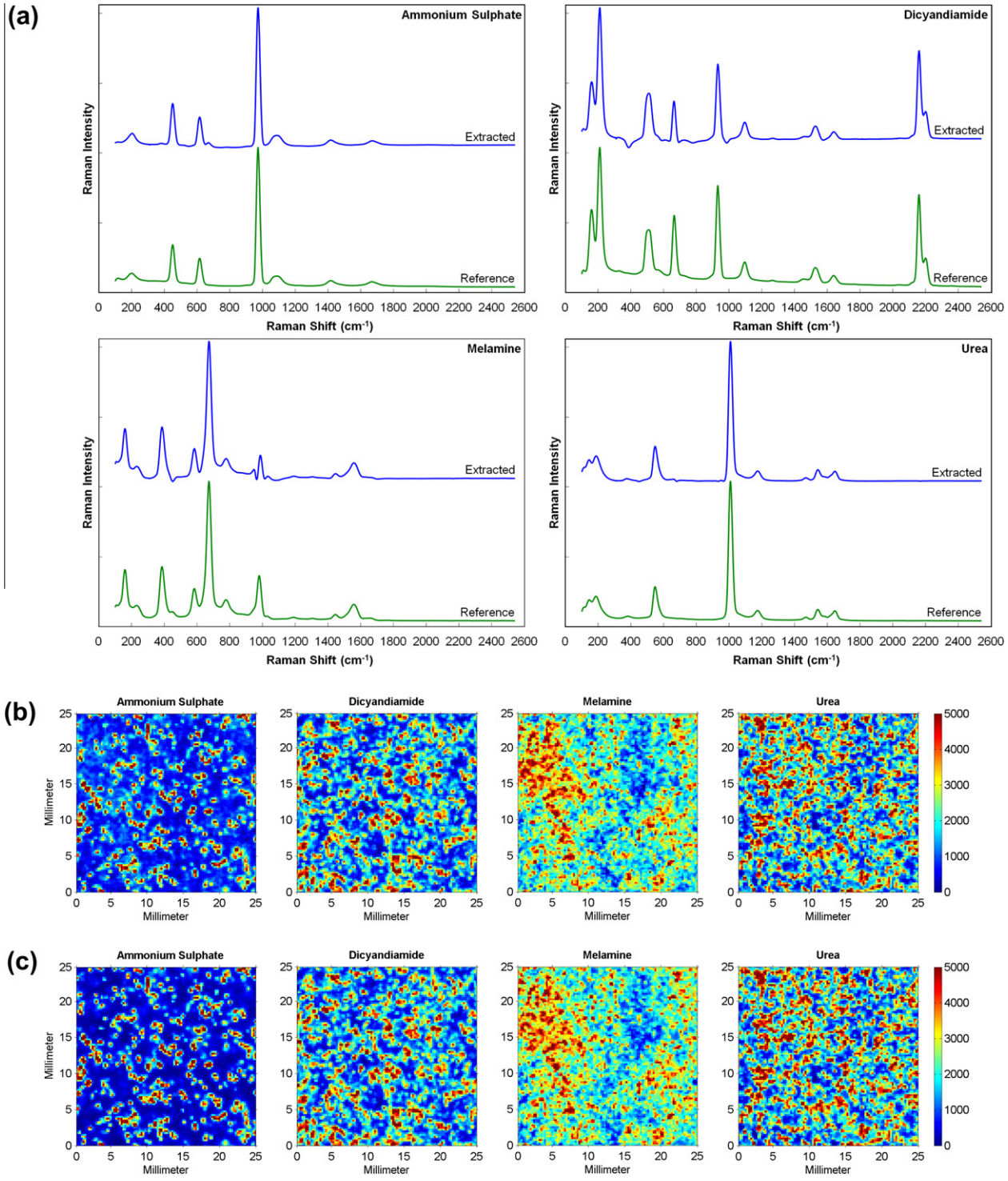


**Fig. 3.** Self-modelling mixture analysis for mixed chemical adulterants: (a) pure component spectra and (b) contribution maps. Contribution maps from classical least squares using reference spectra of adulterants are shown in (c).

from SMA using eight components. The other four spectra (not shown) were not recognizable and they likely represented the residual noise generated from the matrix decomposition. Spectra were also extracted from SMA using three to seven pure components. The first four resolved spectra from using four, five, six, and seven components were similar to those obtained from eight components. However, when only three components were used, the Raman peaks of one adulterant (melamine in this case) were found in the three resolved spectra (that were otherwise more representative of ammonium sulphate, dicyandiamide, and urea), making these spectra less pure than those from SMA using no fewer than four components. These results suggest that a sufficiently large number of pure components (no fewer than the number of constituents) are necessary for SMA to effectively identify all possible constituents in a mixture.

The contribution maps of each identified adulterant from self-modelling mixture analysis and from classical least squares are shown in Fig. 3b and c, respectively. The score values in the

contribution images are proportional to the actual concentrations of each chemical. Thus the pixels with high intensities likely represent the adulterant particles in each map. The general patterns of the contribution maps from SMA are similar to the corresponding reference maps from CLS, owing to the similarities between the pure component spectra and the reference spectra (Fig. 3a). The above results on the pure component spectra and the contribution maps prove that SMA is capable of identifying and locating the individual compositions in the mixture of the four adulterants based on their unique Raman characteristics.

### 3.3. Identification of multiple adulterants in dry milk

Fig. 4 shows Raman spectra and images of a milk-adulterant mixture containing 5.0% of each of the four adulterants. Both the fluorescence signals from the dry milk and the Raman peaks of the individual adulterants were observed in the spectra of the mixture sample. The Raman peaks with relatively low intensities were not as prominent as those observed for the four-adulterant mixture without milk powder (Fig. 2a) since some of these peaks were overwhelmed by the fluorescence background created by the milk. Raman images at four selected peak positions (i.e., 212 $cm^{-1}$ for dicyandiamide, 673 $cm^{-1}$ for melamine, 973 $cm^{-1}$ for ammonium sulphate, and 1009 $cm^{-1}$ for urea) and a position without Raman signals (i.e., 1800 $cm^{-1}$) are shown in Fig. 4b. Similar to the images of the four-adulterant mixture in Fig. 2b, the single-band images at the Raman peak positions reveal the possible existence of the multiple adulterants, as visualised by the bright image pixels at different wavenumbers. The image at 1800 $cm^{-1}$ lacked useful features due to the absence of Raman signals at 1800 $cm^{-1}$. It should be noted that the spectra and the images shown in Fig. 4 were from the mixtures with the highest concentration of the adulterants prepared in this study (5.0%). The Raman signal intensities and the numbers of bright pixels observed for the other concentration levels (i.e., 0.1%, 0.2%, 0.5%, 1.0%, and 2.0%) were generally lower than those for the 5.0% samples.

The pure component spectra extracted from SMA for the milk-adulterant mixtures at six concentration levels are shown in Fig. 5a. The resolved spectra were grouped based on their identifications using the SID values to the reference spectra. The associated reference spectrum is also plotted in each group for the purpose of comparison. As shown in the figure, Raman spectra of the four individual adulterants were successfully retrieved from the milk-adulterant sample spectra at all the concentration levels. In each group, the extracted spectra in the concentration range from 0.2% to 5.0% are generally similar. The four component spectra of the 0.1% sample appear noisy due to the relatively weak scattering signals from the small amount of the adulterant particles, although the overall Raman features are not significantly affected. The component spectra in Fig. 5a were identified and selected from SMA using eight components. Unlike the spectra extracted for the sample mixed with only the four adulterants and no milk (Fig. 3a),

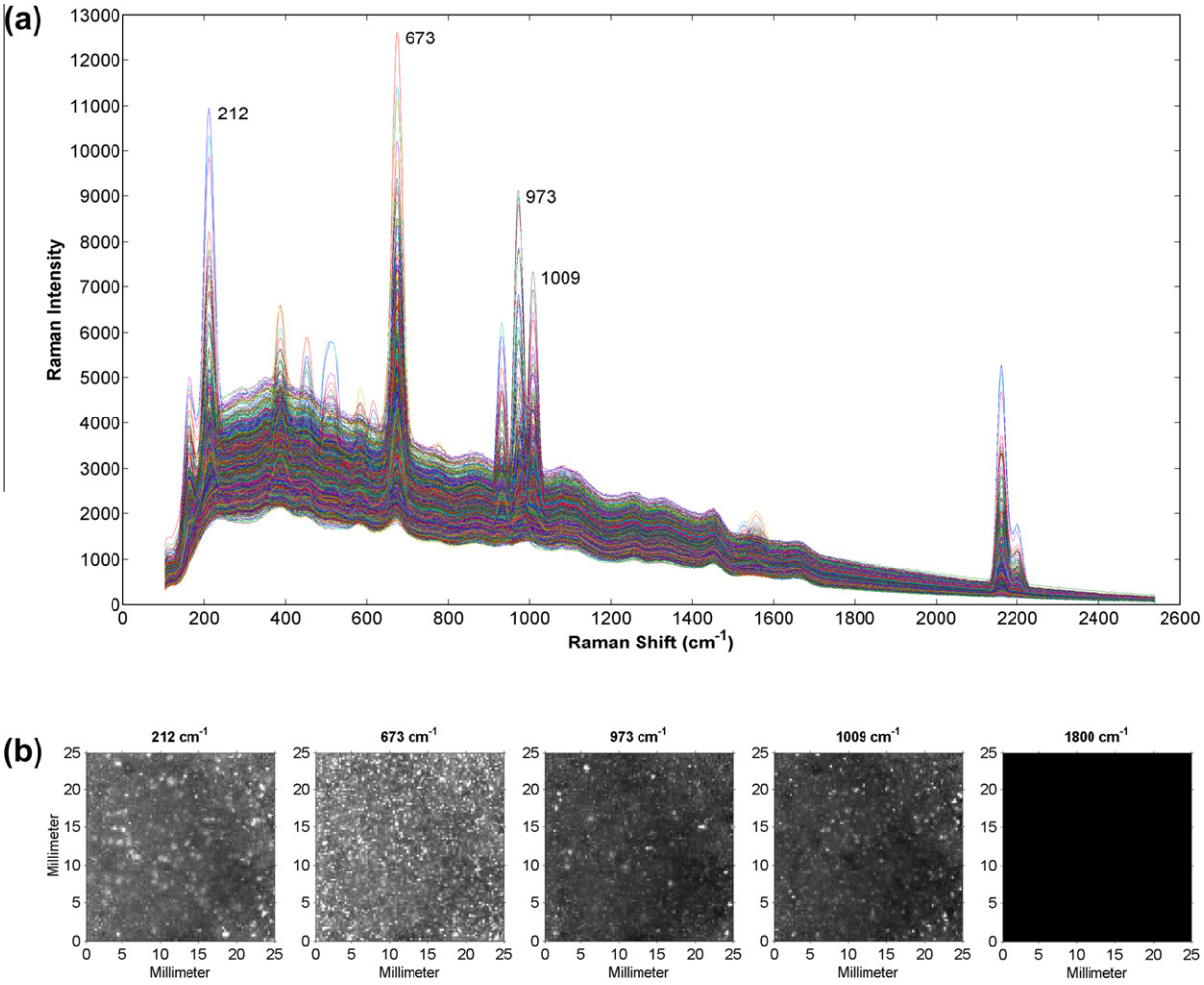


**Fig. 4.** Raman characteristics of dry skim milk mixed with four chemical adulterants (ammonium sulphate, dicyandiamide, melamine, and urea) at a concentration of 5.0% for each adulterant: (a) original spectra and (b) images at selected wavenumbers.

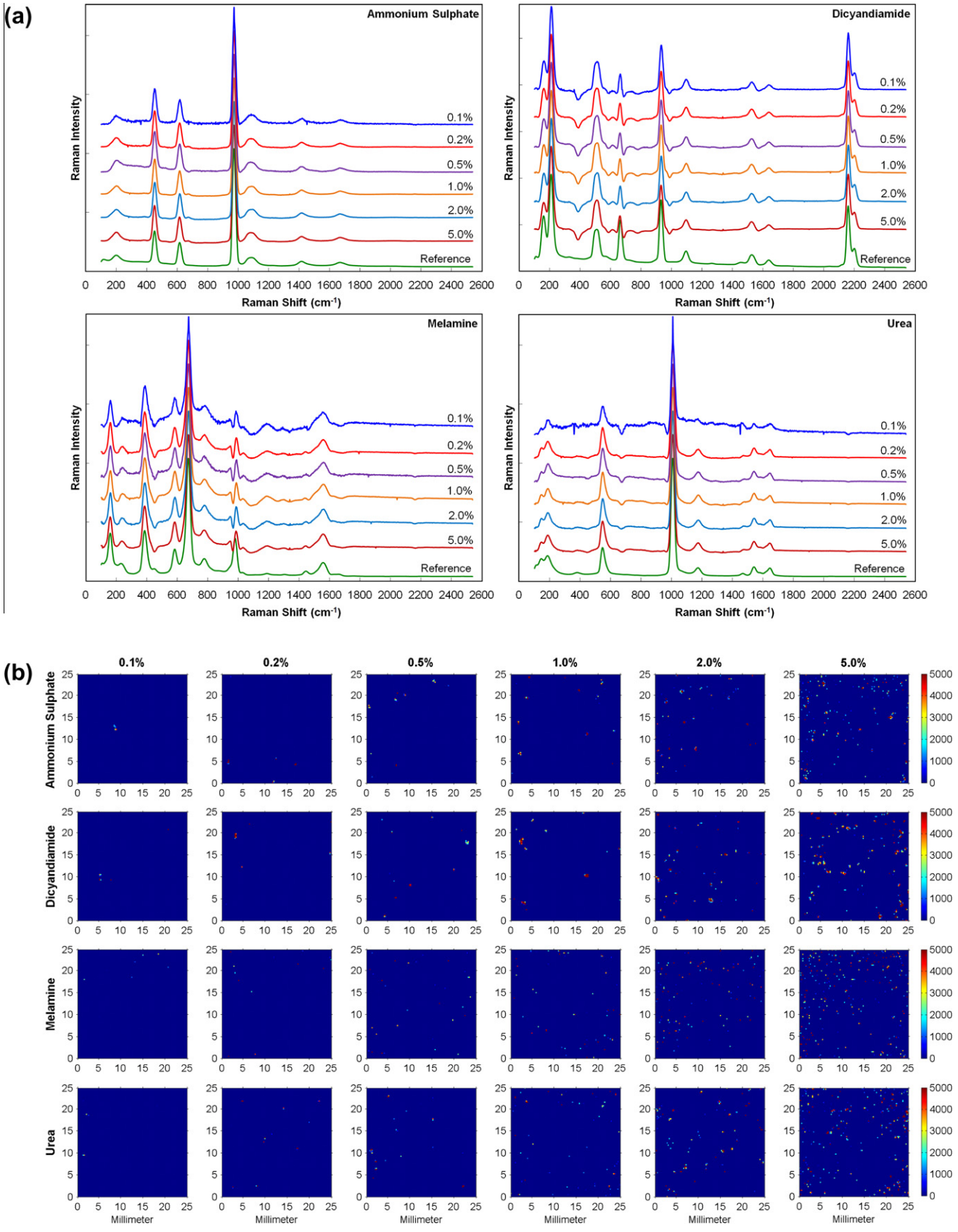


**Fig. 5.** Self-modelling mixture analysis for milk-adulterant mixtures: (a) pure component spectra and (b) contribution maps.

some adulterant spectra for the milk-adulterant mixtures appeared to show random features after the fourth component, especially for the low-concentration samples. The reason for this is that some Raman peaks of the dry milk were also recognized as pure components by SMA and appeared in the first four component spectra. The component spectra from the dry milk were generally

not identifiable since constituent ingredients of the dry milk are in an integrated form instead of separate powders. For example, no component spectra of lactose were found even though some Raman peaks of lactose were observed for the dry milk (Fig. 1a). For all the samples tested in this study, no component spectra of the adulterants were identified after the eighth component. Hence eight components were used in SMA for all the samples. These results confirm that a sufficiently large number of pure components are crucial for self-modelling mixture analysis, especially when dealing with samples of complicated compositions.

The results above were from one out of three sets of the milk-adulterant mixtures. Results from the other two sets of the samples were generally similar to those demonstrated in Fig. 5a, except that one 0.1% sample only generated three identified component spectra of the adulterants (i.e., dicyandiamide, melamine, and urea) rather than four. Ammonium sulphate was not identified in SMA, and this sample was the only one (out of 18) that was not detected as containing four types of the adulterants. The possible explanations for this are that either this one-third portion of the original mixture, after mixing and separation, simply happened to have an extremely low amount of ammonium sulphate (compared to the other two portions), or the ammonium sulphate particles in this portion happened to be located at the bottom of the sample when it was imaged. The thickness of each sample was approximately 5 mm, which might have been enough to prevent the laser from penetrating to reach the particles at the bottom. A thin sample layer would be ideal for detecting adulterant particles in dry milk. Dividing each sample into three parts in this study was an effort to increase the sampling area and reduce the chance of missing the adulterants at the bottom. Under the same experimental settings (e.g., spatial resolution and exposure time), larger sampling area means longer scan time, especially for the two-dimensional scan conducted in the point-scan system. A high-throughput inspection system, such as a line-scan Raman imaging system using a line laser, can scan the large-area sample more efficiently and thereby greatly reduce the sampling time and the possibility of missing the adulterant particles in a thick sample layer. For example, the scan time can be reduced from 120 m (10,000 scans) using the point-scan method to 1.2 m (100 scans) using the line-scan method, assuming that the scan speed is same for the same step size.

The Raman spectrum of homogenized whole milk powder (data not shown) was similar to that of the skim milk powder (Fig. 1a).

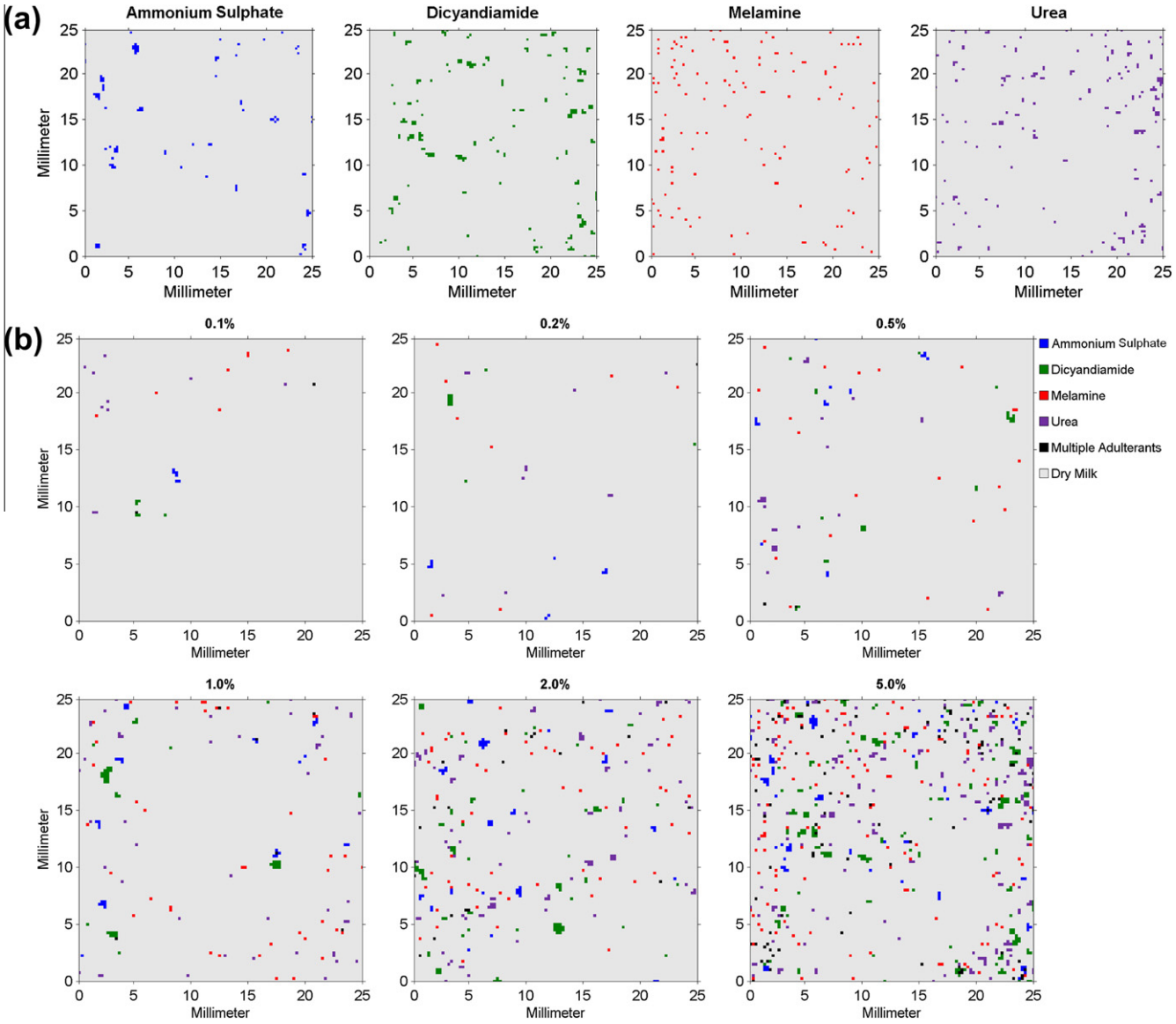


**Fig. 6.** Chemical images of (a) individual adulterants in dry skim milk with the concentration of 5.0% and (b) multiple adulterants in dry skim milk with six different concentrations.

Two small Raman peaks were observed for the whole milk powder at 1305 and 1739 $cm^{-1}$, which were not observed for the skim milk powder and may be attributed to the fat in the whole milk powder. Similar pure component spectra were obtained from the mixture sample containing whole milk powder mixed with the four adulterants at 0.1% for each (results not shown). The two peaks from the whole milk powder did not affect the detection of the four adulterants because the adulterants did not show Raman peaks at 1305 and 1739 $cm^{-1}$. Therefore, this method for simultaneous detection of multiple adulterants can be used for both skim and homogenized whole milk powder. Further testing is anticipated to confirm that the method is equally effective for dry milk powder of intermediate fat contents, such as low-fat and reduced-fat milk.

### 3.4. Spatial mapping of multiple adulterants in dry milk

Fig. 5b shows the contribution images from SMA for the four identified adulterants at six concentration levels in the dry milk. The six samples correspond to the spectra shown in Fig. 5a, and all the images are presented in the same intensity scale for the purpose of direct comparison. In general, the score values in the contribution images reflect the real concentrations of the chemical adulterants. A visual inspection of all 24 contribution maps reveals that the numbers of high-intensity pixels for the four adulterants are roughly at the same level at each concentration, and the pixel numbers gradually increase with the rising concentration of the adulterants. The pixels with the high score values are likely the adulterant particles. To enhance the contrast for the adulterant particles, binary images were generated using a simple thresholding method. Four binary images corresponding to the four adulterants in the 5.0% sample in Fig. 5b are demonstrated in Fig. 6a. A threshold value of 1000 was used to remove the background of the dry milk. The threshold value was determined based on the histograms of the contribution images, in which the majority of the pixels had low score values; these low-score pixels were consequently converted to the background pixels. Pixels with intensities higher than the threshold were recognized as the adulterant particles. The four binary images were then combined to form a single image (5.0% sample in Fig. 6b). Some pixels were locations of overlap due to the possibility that more than one type of adulterant particle was imaged within the one pixel area ($0.25 \times 0.25$ $mm^2$), and so these pixels were labelled as "Multiple Adulterants" regardless of which adulterant type was contained within.

The same procedures were applied to the other contribution maps in Fig. 5b, and the final combined images for the six concentration levels are shown in Fig. 6b. These combined images can be regarded as Raman chemical images since they provide a clear view of the identification and distribution of the multiple adulterants in the milk powder. The numbers of pixels in each chemical image are generally consistent with the concentrations of the adulterants. Morphological features of the adulterant particles can also be visualised in the chemical images. For example, based on the visual inspection, dicyandiamide has the largest particle size among the four adulterants mixed with the dry milk. This was confirmed in the chemical images in that the areas of the connected pixels of dicyandiamide are generally larger than those of the other three adulterants. The chemical images in Fig. 6b correspond to the six mixtures shown in Fig. 5. Similar results were obtained from the other two sets of the samples. The spatial and spectral information in the hyperspectral Raman images were successfully used to answer the question of "where is what" in detecting the four types of adulterants in the dry milk. Reference Raman spectra of new adulterants can be added to the spectral library for inspecting for more types of the adulterants in the milk powder. The Raman chemical imaging technique has great potential to be extended to authenticate other powdered food and food ingredients.

## 4. Conclusion

Rapid and accurate authentication of food ingredients is important for food safety and quality evaluation. This study demonstrated that Raman chemical imaging coupled with proper mixture analysis algorithms can be used for simultaneous detection of multiple adulterants in milk powder. The hyperspectral Raman imaging system is capable of acquiring sufficient spectral and spatial information to identify and map the adulterant particles mixed into the dry milk. Using a reasonably large number of pure components, self-modelling mixture analysis (SMA) was able to extract Raman spectra of all four adulterant types (i.e., ammonium sulphate, dicyandiamide, melamine, and urea) in the dry milk at all concentration levels from 0.1% to 5.0%. The pure component spectra were identified using their spectral information divergence values to the reference spectra of the adulterants. The contribution images from SMA reflected the real concentrations of the chemical adulterants. The view of the adulterant particles was enhanced in the binary images that were converted from the contribution maps. Raman chemical images, which were generated by combining the binary images of the individual adulterants, can be used to visualise identification and spatial distribution of the multiple adulterant particles in the dry milk. Since the adulterant detection method is effective for both skim and homogenized whole milk powder, it is anticipated that further testing will show the method to be valid for other milk powder products of varying fat content. A thin sample layer is ideal for the adulterant inspection since the adulterant particles can be missed in a thick sample layer. Developing a high-throughput line-scan Raman imaging system, which can scan a larger sample area, such as that for a sample mixture that is spread more thinly, and reduce overall sampling times, is planned as the next step in this research.

## References


Almeida, M. R., Oliveira, K. D., Stephani, R., & de Oliveira, L. F. C. (2011). Fourier-transform Raman analysis of milk powder: A potential method for rapid quality screening. *Journal of Raman Spectroscopy, 42*, 1548–1552.

Belloque, J., & Ramos, M. (1999). Application of NMR spectroscopy to milk and dairy products. *Trends in Food Science & Technology, 10*, 313–320.

Borin, A., Ferrao, M. F., Mello, C., Maretto, D. A., & Poppi, R. J. (2006). Least-squares support vector machines and near infrared spectroscopy for quantification of common adulterants in powdered milk. *Analytica Chimica Acta, 579*, 25–32.

Chang, C.-I. (2000). An information theoretic-based approach to spectral variability, similarity and discriminability for hyperspectral image analysis. *IEEE Transactions on Information Theory, 46*, 1927–1932.

Chao, K., Qin, J., Kim, M.S., & Mo, C.Y. (2011). A Raman chemical imaging system for detection of contaminants in food. In: *Proceedings of SPIE* (Vols. 8027, 802710). Defense and security symposium 2011, FL. USA: Orlando.

Hau, A. K.-C., Kwan, T. H., & Li, P. K.-T. (2009). Melamine toxicity and the kidney. *Journal of the American Society of Nephrology, 20*, 245–500.

Hu, F., Furihata, K., Kato, Y., & Tanokura, M. (2007). Nondestructive quantification of organic compounds in whole milk without pretreatment by two-dimensional NMR spectroscopy. *Journal of Agricultural and Food Chemistry, 55*, 4307–4311.

Lu, C. H., Xiang, B. R., Hao, G., Xu, J. P., Wang, Z. W., & Chen, C. Y. (2009). Rapid detection of melamine in milk powder by near infrared spectroscopy. *Journal of Near Infrared Spectroscopy, 17*, 59–67.

McGoverin, C. M., Clark, A. S. S., Holroyd, S. E., & Gordon, K. C. (2010). Raman spectroscopic quantification of milk powder constituents. *Analytica Chimica Acta, 673*, 26–32.

Moros, J., Garrigues, S., & de la Guardia, M. (2007). Evaluation of nutritional parameters in infant formulas and powdered milk by Raman spectroscopy. *Analytica Chimica Acta, 593*, 30–38.

Okazaki, S., Hiramatsu, M., Gonmori, K., Suzuki, O., & Tu, A. T. (2009). Rapid nondestructive screening for melamine in dried milk by Raman spectroscopy. *Forensic Toxicology, 27*, 94–97.

Qin, J., Chao, K., & Kim, M. S. (2010). Raman chemical imaging system for food safety and quality inspection. *Transactions of the ASABE, 53*, 1873–1882.

Qin, J., Chao, K., & Kim, M. S. (2011). Investigation of Raman chemical imaging for detection of lycopene changes in tomatoes during postharvest ripening. *Journal of Food Engineering, 107*, 277–288.

Vajna, B., Patyi, G., Nagy, Z., Bodis, A., Farkas, A., & Marosi, G. (2011). Comparison of chemometric methods in the analysis of pharmaceuticals with hyperspectral Raman imaging. *Journal of Raman Spectroscopy, 42*, 1977–1986.

Windig, W., & Guilment, J. (1991). Interactive self-modeling mixture analysis. *Analytical Chemistry, 63*, 1425–1432.

Wise, B.M., Gallagher, N.B., Bro, R., Shaver, J.M., Windig, W., & Koch, R.S. (2006). *PLS_Toolbox Version 4.0 for use with MATLAB*. Wenatchee, WA, USA: Eigenvector Research, Inc.